

AD-268652

IMPROVEMENT OF THE USEFULNESS
OF PYROLYTIC GRAPHITE
IN ROCKET MOTOR
APPLICATIONS

Quarterly Progress Report
September through November, 1961

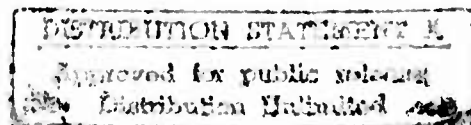
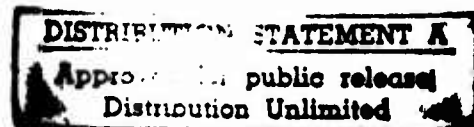
Contract No. DA-36-034-ORD-3279RD
Project No. TB4-004

Contributors:

J. D. Batchelor
E. F. Ford
S. W. McCormick
E. L. Olcott
R. K. White

December 15, 1961

Atlantic Research Corporation
Alexandria, Virginia



CONTENTS

	<u>Page</u>
I. INTRODUCTION	1
II. SUMMARY AND CONCLUSIONS	1
III. DEPOSITION PROCESS STUDIES	2
IV. MECHANICAL DESIGN STUDIES	4
V. MOTOR FIRING TESTS	8
VI. LITERATURE CITATIONS	10

List of Tables

Table I.	Deposition Runs at Lower Temperatures
Table II.	Contoured Nozzle Test Piece Fabrication
Table III.	Motor Test Firings with 6500°F Propellant

List of Figures

Figure 1.	Microstructure of Coatings Produced from Methane at 1300-1700°C
Figure 2.	Microstructure of Coatings Produced from Propane at 1300°C
Figure 3.	Elongation in a Composite Bar (Model)
Figure 4.	Equilibrium Diagram for Composite Bar (Model)
Figure 5.	Calculated Shear Stress Distribution for Various Length Composite Bars
Figure 6.	Segmented Test Nozzle Before Assembly for Test with 6500°F Propellant
Figure 7.	Shadowgraph of Nozzle from Firing PYB-2 with 6500°F Propellant

I. INTRODUCTION

This report describes the work performed during the quarter from September 1, 1961, through November 30, 1961. During this period work was carried out in three areas of study: (1) deposition process studies, (2) mechanical design analysis, and (3) motor firing tests of pyrolytic graphite nozzles.

A conference was held during this quarter with Mr. C. H. Martens, ARGMA, Project Engineer, and Mr. Irving Kahn, OMRO, Watertown Arsenal, in which the objectives of this program were reviewed. The sponsors requested that principal emphasis for the remainder of this program be placed on the determination of the performance capabilities of a good grade of pyrolytic graphite in solid-propellant rocket motor nozzles under a variety of environmental conditions. A lesser emphasis is to be placed on work aimed at producing an optimum grade of pyrolytic graphite. Thus, in the current quarter and in the future work, preparation of nozzle test pieces and the motor test firing of these nozzles will receive priority over the process and design studies. Some time should be available without impeding our nozzle test work to pursue promising methods of process or design improvements.

II. SUMMARY AND CONCLUSIONS

Research on this program has continued in three phases consisting of deposition process studies, mechanical design analysis, and preparation and motor test firing of pyrolytic graphite coated nozzle inserts. The deposition process studies have shown that pyrolytic graphite coatings can be prepared in the temperature range from 1300 to 1700°C. However, coatings prepared below 1500°C are very coarse grained. The effect of surface pretreatment and substrate purity on the quality of pyrolytic graphite coatings made at temperatures in the 1300 to 1700°C range will be examined. The use of such lower deposition temperatures can markedly reduce the complexity and expense of the process as well as possibly produce coatings of different properties.

The mechanical design analysis has continued to be concerned with the calculation of the residual thermal stresses formed in the coated bodies during the deposition process. One analysis, based on a simple but logical model, has been completed which shows qualitatively the effect of axial length of the coated part on the magnitude and distribution of the shear stresses at the coating-substrate interface. Substantial progress has been made on the exact solution of a more complex mathematical model. A re-examination of the extent to which these analyses should be followed in this program is underway.

The motor firing program has moved from tests in a 5600°F propellant, for which pyrolytic graphite shows excellent serviceability, to a 6500°F propellant which yields a much more severe environment. The coating was lost in nine seconds from the first test piece fired with the 6500°F propellant as a result of excessive motor pressure. A second test piece displayed a very good erosion rate of 0.48 mil/sec in a firing at normal high pressure. This erosion rate is superior to any other graphitic material tested to date.

III. DEPOSITION PROCESS STUDIES

The study of the deposition process variables for making pyrolytic graphite coatings on graphite substrates has been carried out and described in previous reports^{1, 2} to the point where a good grade coating can be prepared reproducibly. Since optimization of the process conditions has been assigned reduced priority in the program, further work will emphasize those changes in process conditions which might produce substantial reductions in the cost or complexity of the production process or which may produce pyrolytic graphite of markedly different physical or chemical properties. One method by which the deposition process could be substantially simplified would be the reduction of the deposition temperature. Power requirements, of course, would decrease and furnace requirements would be simpler. Residual stresses should be somewhat less and anisotropy should decrease. Although the effect of decreased anisotropy is not completely clear, one advantage to be expected is greater transverse strength.

To evaluate the possibility of preparing pyrolytic graphite coatings at lower temperatures, a series of deposition runs was made with substrate temperatures in the range 1100-1700°C. The standard cylindrical substrate of 1 inch inside diameter was used in each run. The total gas flow for each run was 20 SCFH with 10 per cent of the flow being introduced outside of the cooled gas injector. The gas flowing outside the injector was argon only and was the quantity found to be optimum for deposition runs at 2000°C. No effort has yet been made to determine the proper distribution of gas within and outside of the injector for low temperature deposition. If a desirable coating can be achieved at a lower temperature, the preferred gas flow and distribution will be determined.

The results of the low temperature deposition tests and the conditions used in each run are shown in Table I. It is apparent that the deposition rate is substantially reduced as the substrate temperature is reduced. The absolute values of the deposition rate apply at the section of maximum coating thickness, and no attempt was made to obtain uniform coatings. The trend with reduced temperature is clear, however.

At 1100°C no measurable coating was found after the two-hour deposition run. Propane was substituted for methane in Runs 40 and 41 to see if the less thermally stable propane would produce a more rapid coating at 1300°C. The observed deposition rate was proportional to the atomic concentration of carbon in the source gas and indicated no increased deposition rate from the use of propane.

The effect of reduced deposition temperature on the microstructure of the coatings can be seen in Figures 1 and 2. Lowering the substrate temperature encourages the formation of large, erratic cone structures. Such a coating is likely undesirable because of the surface roughness and the greater number of separations within the cones. At 1300°C the coatings produced from either methane or propane show erratic cone growth. At 1500°C and 1700°C the coatings are much smoother and finer grained. At substrate temperatures up to about 1500°C the catalytic effects of the substrate surface presumably assume greater importance in determining the local deposition rates than at higher temperatures. For this reason, a series of tests will be made to examine the effect of surface

pretreatment and the effect of using a high-purity graphite substrate on the quality of coatings made at low substrate temperatures. Nozzle test sections of the best microstructure that can be produced at lower deposition temperatures will be included in the motor firing program.

IV. MECHANICAL DESIGN STUDIES

In the earlier reports on this program^{1, 2} the stress problems involved in using pyrolytic graphite as a coating on a commercial graphite substrate have been discussed and the general equations for the stress-strain relationships in pyrolytic graphite were presented. Stresses can arise in each of the following categories:

- (a) Residual or "built-in" stresses from manufacture,
- (b) Thermal stresses in service, and
- (c) Pressurization or other stresses in service.

Mismatch of the thermal properties between pyrolytic graphite and most substrate materials and the substantial thermal anisotropy of the pyrolytic graphite combine to make the thermal stresses (a) and (b) of major importance. The pressure stresses (c) may be significant, but sufficient rigidity can generally be supplied by the substrate to minimize any failure related to this source of stress.

During the current quarter a continued study of the thermal stress problems in pyrolytic graphite coatings has been made. Since the exact treatment of even an idealized (and simplified) composite system having the actual nozzle contour may be beyond the scope of this program, a simple, logical model was examined first to determine the manner in which the shearing stresses at the coating-substrate interface can be expected to vary within coated nozzles of various lengths.

An axial rocket nozzle coated with pyrolytic graphite can be considered, for some purposes, as a thick composite two-component bar in which shear

deformation (but no bending) is caused by the difference between the thermal expansion coefficients of the component materials. A simple approximate theory gives a reasonable picture of the distribution of interface shearing stresses in such a composite bar.

Let the composite bar have the length $2L$. Let the component bars have cross-section areas A_1 and A_2 , elastic moduli E_1 and E_2 , and thermal expansion coefficients α_1 and α_2 , respectively. Let the surface of contact between the two components have the width S .

The composite bar is free of stresses at the temperature $T = 0$. At other temperatures, differential thermal expansion causes initially plane cross-sections to become warped. Let us set up a coordinate system (x, y, z) with the x -axis parallel to the main axis of the composite bar with the origin at the center of the bar. Let u, v, w , be displacements parallel to the x, y , and z axes, respectively. We will assume that the deformation of the composite bar can be described adequately by $u = U(x) + D(x) \cdot F(y, z)$; $v = w = 0$. Here, $U(x)$ is a displacement parallel to the main axis of the composite bar and uniform over each cross-section of the bar; $D(x) F(y, z)$ is a shearing distortion with an amplitude $D(x)$ which varies along the length of the bar.

A mean interface shearing stress $\bar{\tau}$ acts across the surface of contact between the two components. $\bar{\tau}$ will be proportional to $D(x)$;

$$\bar{\tau} = K_{\tau} D(x), \quad (1)$$

where K_{τ} is a coefficient which depends on the distortion function $F(y, z)$. For component bar number 1, we define a "mean elongation"

$$\bar{\epsilon}_1 = K_1 \frac{\partial D}{\partial x} + \frac{\partial U}{\partial x} \quad (2)$$

(see Figure 3). Here the coefficient K_1 is chosen so that the "stress-strain" relation

$$\bar{\sigma}_1 = E_1 \bar{\epsilon}_1 - E_1 \alpha_1 T \quad (3)$$

is valid. ($\bar{\sigma}_1$ is the mean normal stress over the cross-section area, A_1 .)

Similarly, we write

$$\bar{\epsilon}_2 = K_2 \frac{\partial D}{\partial x} + \frac{\partial U}{\partial x} \quad (4)$$

and

$$\bar{\sigma}_2 = E_2 \bar{\epsilon}_2 - E_2 \alpha_2 T \quad (5)$$

for component bar number 2.

If we consider the translational equilibrium in the x-direction of small sections of the component bars (Figure 4), we find

$$A_1 \frac{\partial \bar{\sigma}_1}{\partial x} + S \bar{\tau} = 0 \quad (6)$$

$$A_2 \frac{\partial \bar{\sigma}_2}{\partial x} - S \bar{\tau} = 0 \quad (7)$$

Finally, since the ends of the composite bar are free, we have

$$\bar{\sigma}_1 = \bar{\sigma}_2 = 0 \quad \text{at} \quad x = \pm L. \quad (8)$$

It can easily be verified that the solution of Equations (1) - (8) is

$$D(x) = \frac{\bar{\tau}}{K_\tau} = \frac{(\alpha_2 - \alpha_1) T}{K_2 - K_1} \frac{\sinh \gamma x}{\gamma \cosh \gamma L} \quad (9)$$

$$U(x) = -\frac{(\alpha_2 - \alpha_1) T}{K_2 - K_1} \frac{\nu_1 K_2 + \nu_2 K_1}{\nu_1 + \nu_2} \frac{\sinh \gamma x}{\gamma \cosh \gamma L} + \frac{\nu_1 \alpha_2 + \nu_2 \alpha_1}{\nu_1 + \nu_2} T x \quad (10)$$

$$\bar{\epsilon}_1 = -\nu_1 \frac{(\alpha_2 - \alpha_1) T}{\nu_1 + \nu_2} \frac{\cosh \gamma x}{\cosh \gamma L} + \frac{\nu_1 \alpha_2 + \nu_2 \alpha_1}{\nu_1 + \nu_2} T \quad (11)$$

$$\bar{\epsilon}_2 = \nu_2 \frac{(\alpha_2 - \alpha_1) T}{\nu_1 + \nu_2} \frac{\cosh \gamma x}{\cosh \gamma L} + \frac{\nu_1 \alpha_2 + \nu_2 \alpha_1}{\nu_1 + \nu_2} T \quad (12)$$

$$\bar{\sigma}_1 = \frac{E_1 \nu_1 (\alpha_2 - \alpha_1) T}{\nu_1 + \nu_2} \left(1 - \frac{\cosh \gamma x}{\cosh \gamma L} \right) \quad (13)$$

$$\bar{\sigma}_2 = -\frac{E_2 \nu_2 (\alpha_2 - \alpha_1) T}{\nu_1 + \nu_2} \left(1 - \frac{\cosh \gamma x}{\cosh \gamma L} \right) \quad (14)$$

where

$$\gamma^2 = \frac{v_1 + v_2}{K_2 - K_1}$$

$$v_1 = \frac{S K_T}{A_1 E_1}$$

$$v_2 = \frac{S K_T}{A_2 E_2}$$

The dimensionless mean interface shear $\frac{\gamma (K_2 - K_1)}{K_T (\alpha_2 - \alpha_1) T} \bar{\tau}$ is of particular

interest. In Figure 5, this quantity is plotted against dimensionless distance, γx , from the bar center for various values of the dimensionless bar half-length, γL . The sign of $\bar{\tau}$ is reversed for negative x . The dotted line is a plot of the maximum interface shear against the bar half-length.

Thus, according to this approximate theory, the maximum interface shear in a composite rocket nozzle will increase with increasing nozzle length, but will become essentially constant for sufficiently long nozzles ($\gamma L > 3/2$). For short nozzles, $\bar{\tau}$ will be proportional to distance from the nozzle center; for long nozzles, $\bar{\tau}$ will be very small in the center portion of the nozzle, but will rise exponentially as the nozzle ends are approached.

An exact treatment of the residual thermal stresses in a pyrolytic graphite layer deposited on a rigid substrate with cylindrical (in the general geometrical sense) surface has been started. For this analysis the elastic anisotropy of the coating has been ignored. The First Annual Summary Technical Progress Report discusses the effect of elastic anisotropy. The following summary describes the status of this analysis.

A perturbation method has been developed for use when the coating thickness, h , is small compared to the smallest radius of curvature of the substrate surface.

Two terms in the perturbation series have been considered in the region near the center of the coating, far from the edges. The first term predicts no shearing stresses at the coating-substrate interface. The second term does predict such shearing stresses, and can be evaluated easily for any

substrate shape provided that the solution of a standard problem involving a single change in substrate curvature is known. This basic solution can be expressed in terms of rather complicated trigonometric integrals, the numerical evaluation of which has not yet been completed.

Only the first term in the series has been considered near the coating edges. Here the stresses in and deformations of the coating can be expanded in a series of eigenfunctions, which can (in principle) be combined to satisfy any set of boundary conditions at the coating edges. It is hoped that these eigenfunctions can be used to evaluate the effect of various edge shapes on the shearing stresses within the coating. The numerical evaluation of the eigenfunctions has not been completed.

A number of factors not considered in the above model, such as coating elastic anisotropy, substrate elasticity, and substrates having solid-of-revolution geometry, are of considerable interest in connection with the general coating problem. However, in view of the mathematical complexity of even the above model, the treatment of other or more general models has been deferred until engineering data are obtained based on the simple model and the mathematical techniques employed have shown their usefulness. At the present time an assessment of the extent to which these analyses can be logically pursued on this program is being made.

V. MOTOR FIRING TESTS

Results reported previously^{1, 2} for the motor testing of pyrolytic graphite coatings have shown the material to be highly serviceable in a 5600°F flame temperature, aluminized Arcite propellant. Consistent with the increased emphasis on the capabilities of a good grade of pyrolytic graphite in a variety of test environments, the motor test program has proceeded to the use of a 6500°F aluminized Arcocel propellant. The arrangement of the three-piece segmented test nozzle was altered so that the pyrolytic graphite coating extends beyond the throat region to prevent excessive erosion of the uncoated parts of the nozzle.

No molded graphite is available which does not erode in the 6500°F propellant when placed near the nozzle throat. Figure 6 is a photograph of a segmented nozzle with a contoured throat section prior to assembly for a test. This segmented design allows a maximum freedom in examining the throat section before, as well as after, the firing test. A tungsten entrance section will be used to prevent erosion in this piece if this becomes necessary to obtain good test firings. Full nozzle test pieces can also be used to prevent test failures caused by inferior materials placed too close to the nozzle throat, but pre-firing examination of the throat section would then be impossible.

Three contoured nozzle test sections were coated during the current period as shown in Table II. The conditions of each deposition were similar to those used to produce a fine-grained coating for test with Arcite 373 (5600°F) propellant. The nozzles coated in Runs N-4 and N-5 were tested in motor firings with Arcocel 163 (4500°F) propellant; the nozzle fabricated in Run N-6 is currently awaiting test. The data from the completed firings are tabulated in Table III.

In firing PYB-1 the pyrolytic graphite coating was lost in about nine seconds. Prior to the loss of the coating the motor burned at an abnormally high pressure level; this excessive pressure undoubtedly contributed to the coating failure. A rather poor joint upstream of the contoured nozzle test piece may also have contributed to this failure. In any case, the performance of the test nozzle in PYB-2 was much better. A uniform erosion of 0.48 mil/sec was measured in this normal high pressure firing. Such performance is excellent under these severe conditions and exceeds the serviceability of any other graphite nozzle tested under comparable conditions. The extent of the nozzle erosion in PYB-2 is shown graphically in the shadowgraph, Figure 7.

VI. LITERATURE CITATIONS

1. Atlantic Research Corporation, "Improvement of the Usefulness of Pyrolytic Graphite in Rocket Motor Applications," First Annual Summary Technical Report, Contract DA-36-034-ORD-3279RD, July, 1961.
2. Atlantic Research Corporation, "Improvement of the Usefulness of Pyrolytic Graphite in Rocket Motor Applications," Quarterly Progress Report, Contract DA-36-034-ORD-3279RD, September, 1961.

Table I. Deposition Runs at Lower Temperatures.

<u>Run^a No.</u>	<u>Temperature (°C)</u>	<u>Carbon Source Gas</u>	<u>Inlet Carbon Source Gas Concentration (per cent)</u>	<u>Mean Deposit Rate^b (mils/hr)</u>	<u>Duration of Run (hours)</u>
36	1700	Methane	5	10.7	2
37	1500	Methane	5	4.5	2
38	1300	Methane	5	2.0	2
39	1100	Methane	5	No deposit	2
40	1300	Propane	2.5	3.0	2
41	1300	Propane	2.5	3.0	4

^aFor all runs:

1. 10 per cent of gas flow entered outside of injector.
2. Substrate surface finish 80 grit.
3. Total gas flow = 20 SCFH.

^bAt cross-section where maximum coating thickness occurs.

Table II. Contoured Nozzle Test Piece Fabrication.

<u>Run No.^a</u>	<u>Gas Preheating Distance^b (inches)</u>	<u>Total Gas Flow (SCFH)</u>	<u>Final Throat Diameter (inch)</u>	<u>Duration of Run (hours)</u>
N-4	4.5	10	0.523	2
N-5	4.5	8	0.531	2
N-6	8.0	8	0.540	2

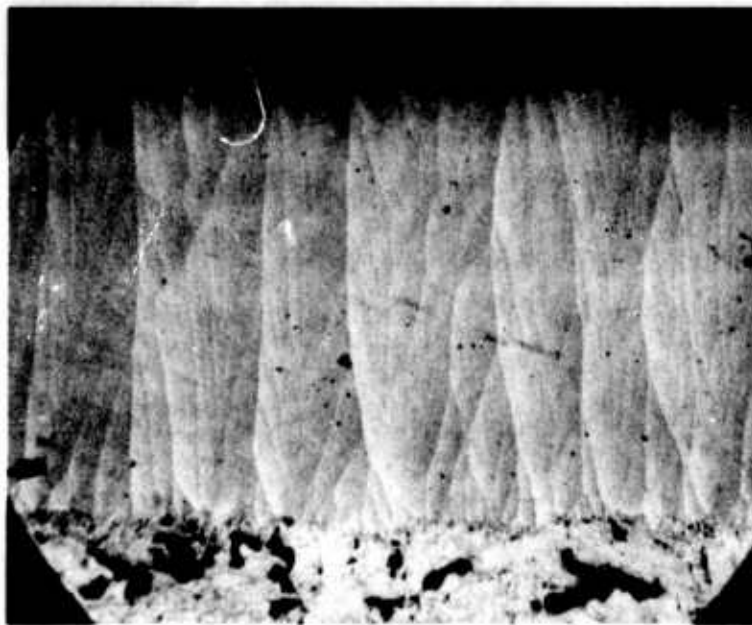
^aData common to each run:
 Temperature - 2000°C
 Carbon source - Methane
 Inert diluent
 Outside injector - 10 per cent
 Inlet carbon
 Source concentration - 5 per cent
 Initial substrate
 Throat diameter - 0.580 inch

^bDistance from tip of cooled gas injector to throat center.

Table III. Motor Test Firings with 6500°F Propellant.

<u>Firing No.</u>	<u>Nozzle Fabrication Run No.</u>	<u>Motor Pressure</u>	<u>Firing Duration (seconds)</u>	<u>Nozzle Diameter (inch)</u>		<u>Nozzle Erosion Rate (mil/sec)</u>
				<u>Before</u>	<u>After</u>	
PYB-1	N-4	Abnormally high	9.0 ^a	0.523	--	--
PYB-2	N-5	Normal high pressure	21.0	0.531	0.551	0.48

^aCoating lost at 9 seconds; motor burned for 65 seconds (total) at reduced pressure.



Run 36

1700°C

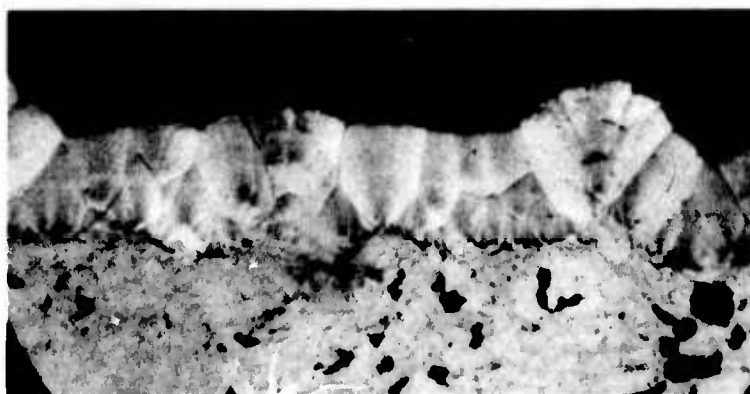
150X



Run 37

1500°C

150X



Run 38

1300°C

150X

Figure 1. MICROSTRUCTURE OF COATINGS
PRODUCED FROM METHANE AT
1300° TO 1700°C.



Run 40

1300°C

150X



Run 41

1300°C

150X

Figure 2. MICROSTRUCTURE OF COATINGS
PRODUCED FROM PROPANE AT
1300°C.

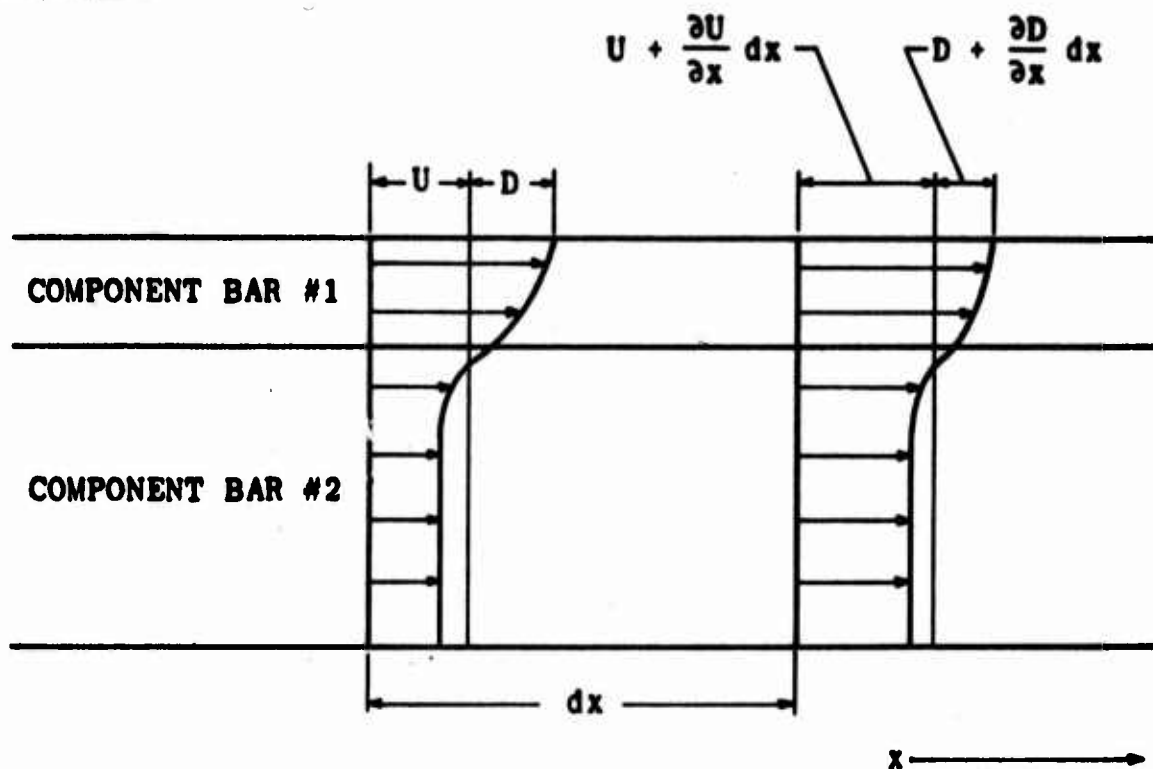


Figure 3. ELONGATION IN A COMPOSITE BAR (MODEL)

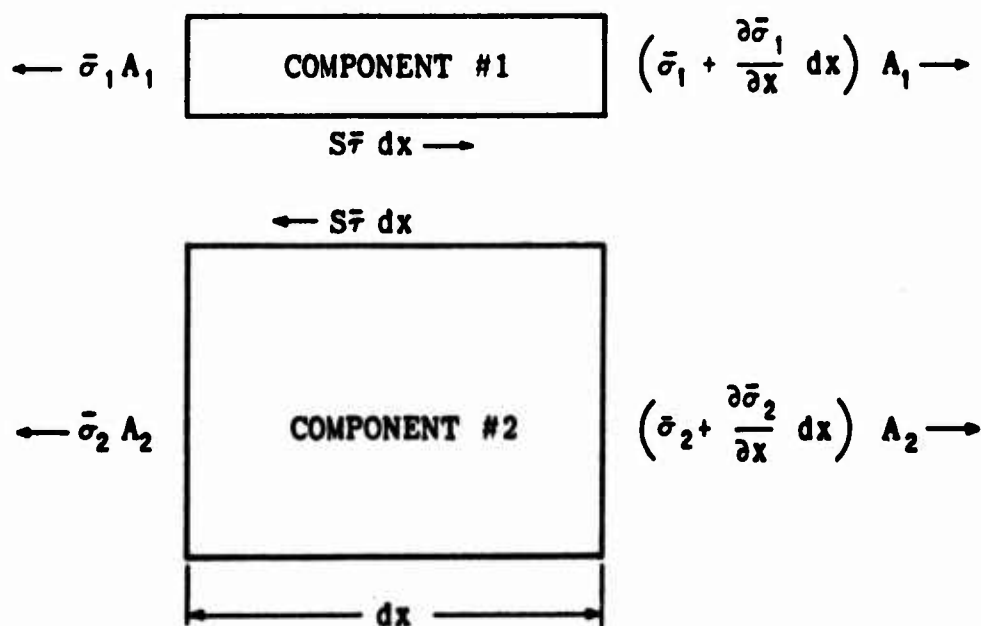


Figure 4. EQUILIBRIUM DIAGRAM FOR COMPOSITE BAR (MODEL)

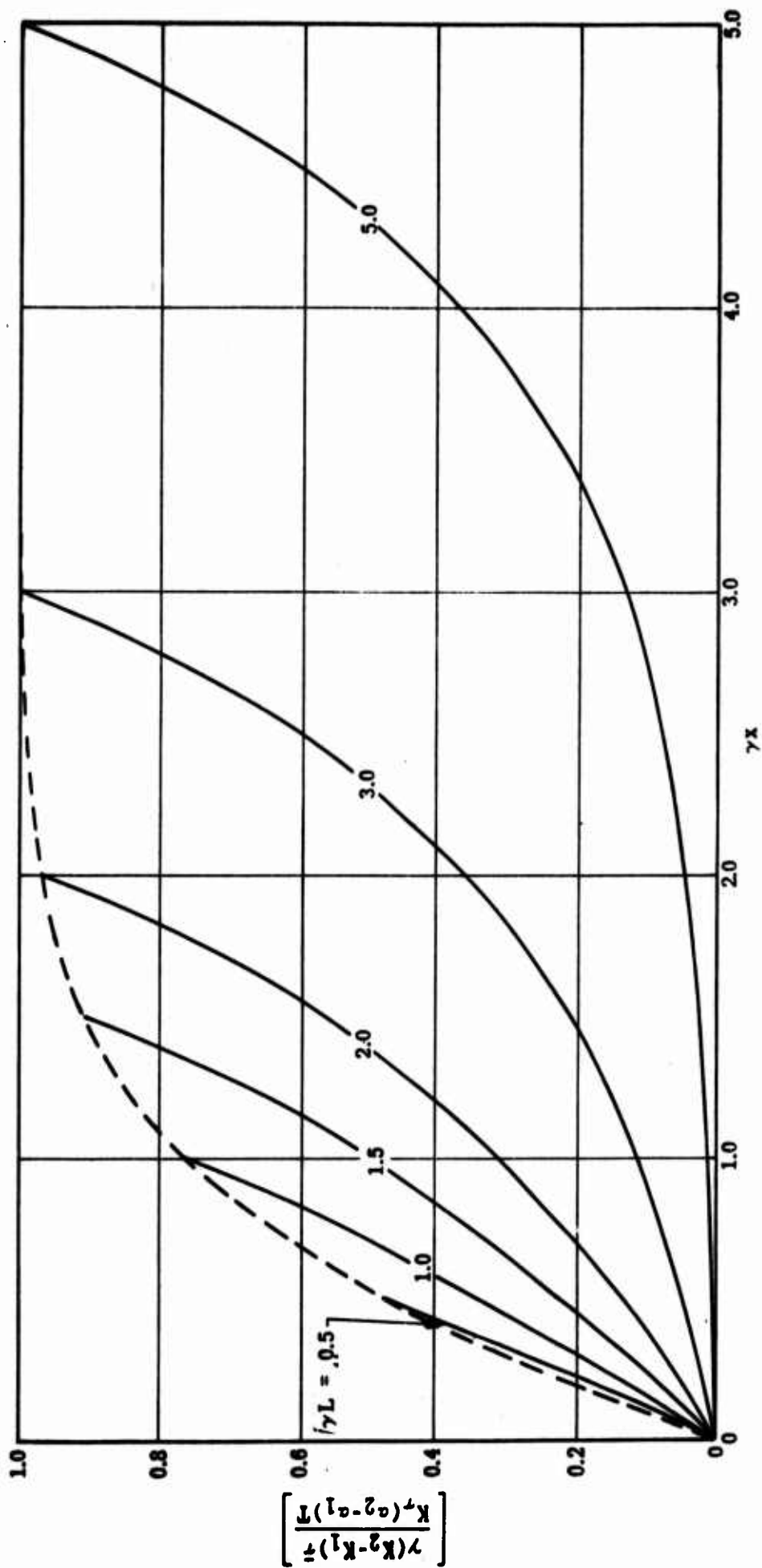
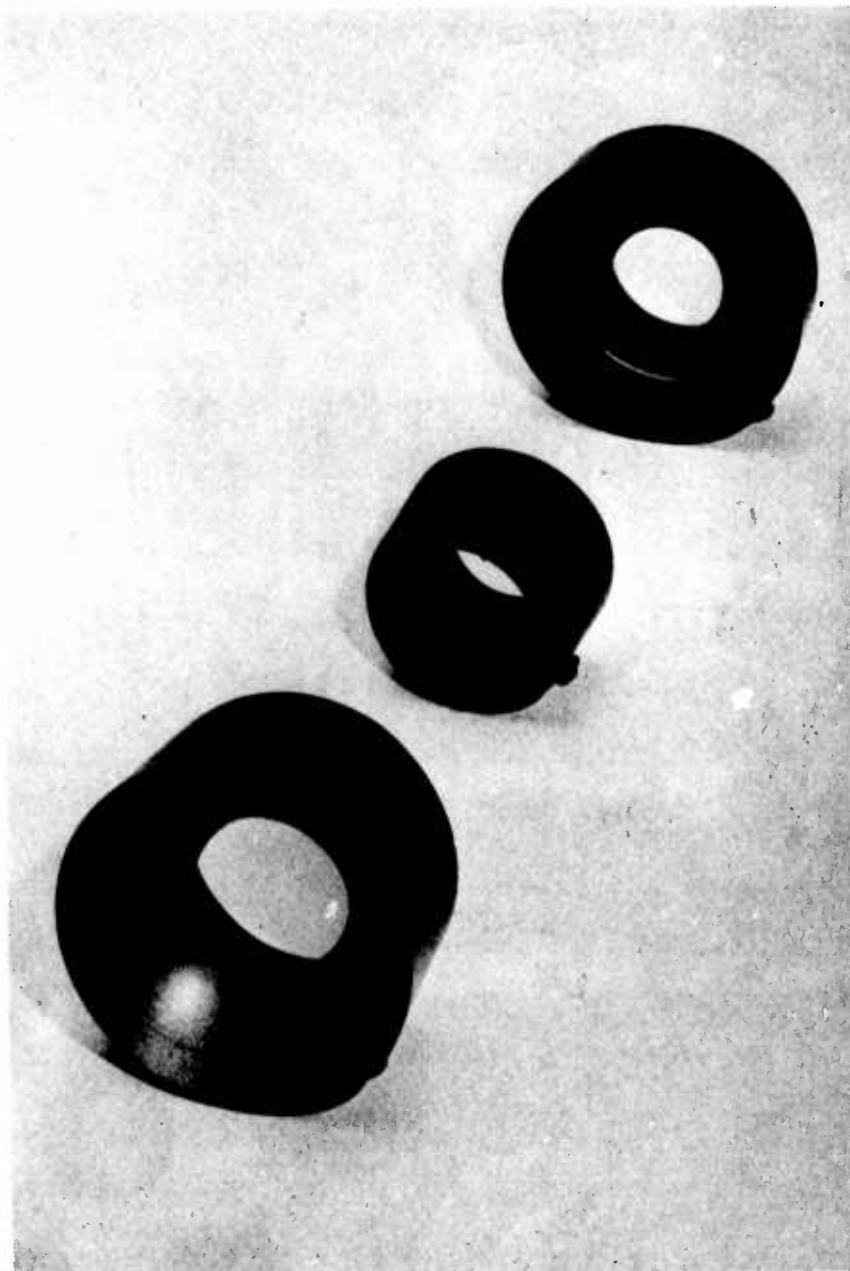
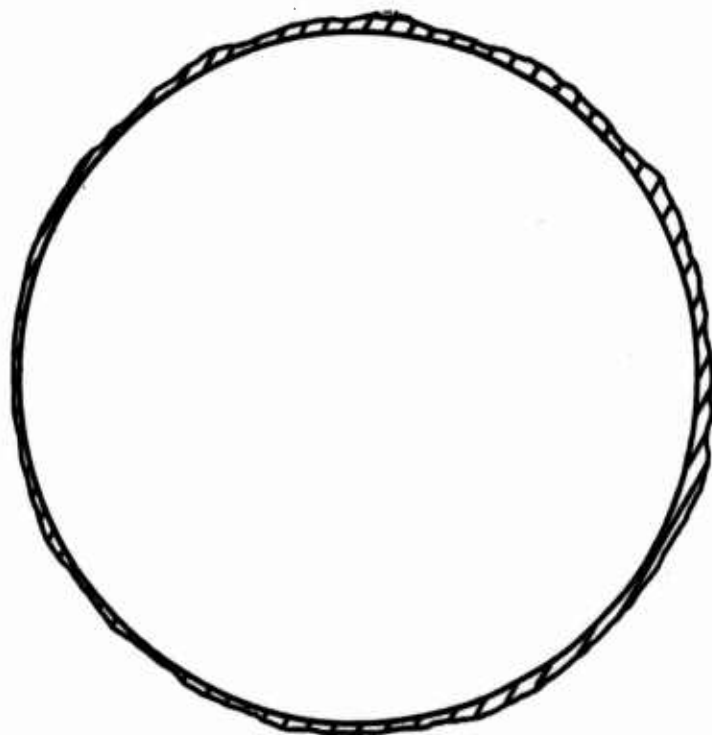


Figure 5. CALCULATED SHEAR STRESS DISTRIBUTION FOR VARIOUS LENGTH COMPOSITE BARS.



**Figure 6. SEGMENTED TEST NOZZLE BEFORE
ASSEMBLY FOR TEST WITH 6500°F
PROPELLANT.**



SCALE: 1 INCH = 0.15 INCH



EROSION

**Figure 7. SHADOWGRAPH OF NOZZLE FROM FIRING
PYB-2 WITH 6500°F PROPELLANT.**